

## SECOND ORDER INTENSITY CORRELATION AND STATISTICAL PROPERTIES OF A SOFT X-RAY FREE ELECTRON LASER\*

Chunlei Li<sup>†</sup>, Tao Liu, Zhichu Chen, Xingtao Wang, Hailong Wu, Jianhui Chen, Bo Liu  
Shanghai Advanced Research Institute, Chinese Academy of Science, Shanghai, China  
also at Shanghai Institute of Applied Physics, Chinese Academy of Science, Shanghai, China

### Abstract

High degree of transverse field coherence is one of the unique properties of an FEL compared with a 3<sup>rd</sup> generation storage ring light source. As a result, the FEL advances the development of innovative research and technology that was not previously feasible. A truly coherent source should be coherent in all orders described from the intensity correlation functions. In this paper, second order intensity correlation of FEL radiation is investigated based on the Hanbury Brown-Twiss intensity correlation method. The statistical properties of radiation produced from SASE was also investigated and compared with the statistical properties of a phase-locked laser. The results show that the statistical properties of a SASE mode behave as a chaotic source, which is significantly different from the properties of a phase-locked laser beam.

### INTRODUCTION

Modern Free Electron Lasers (FEL) have unique properties, such as high brightness (10 orders of magnitude higher than storage rings), ultra-short pulse lengths (<100 fs), and a high degree of transverse coherence [1]. According to Glauber's definition, a fully coherent source is coherent to all orders of intensity correlation [2]. Phase-locked optical lasers are not only coherent in first order, but also in second order which distinguishes the laser source from a chaotic or thermal source [3].

A classical method for characterizing second order coherence is the Hanbury Brown and Twiss (HBT) method developed in 1950s to measure the angular diameter of stars [4-5]. The HBT method is based on the statistical properties of photons and demonstrates a significant difference between a laser and chaotic sources. More recently, HBT intensity correlation has been used to measure the length of electron bunches in synchrotrons [6] and coherence properties of FEL radiation [7-8]. At FERMI, Gorobtsov, et al., explored the statistics properties of radiation produced from both SASE and seeded radiation modes, which showed that the seeded FEL behaves more like a phase-locked laser [9].

In this paper, we present simulation results of the second order intensity correlation for SASE pulses based on the Shanghai Soft X-ray FEL (SXFEL) machine parameters. A statistical analysis of second order intensity correlation function was performed based on ensemble average over many pulses and compared with the properties of a

phase-locked Ti:sapphire laser operating at 800 nm with a pulse length of ~100fs.

### THEORETICAL FRAMEWORK FOR SECOND ORDER INTENSITY CORRELATION AND STATISTICAL PROPERTIES

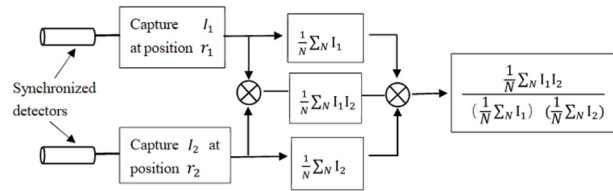


Figure 1: Counting version of intensity interferometer.

The principle of second order intensity correlation is illustrated in Fig. 1. In the simulation, each SASE pulse is measured on a CCD sensor and the two synchronized detectors in Fig. 1 correspond to two pixels on the CCD array. Time synchronization between any two pixels is satisfied by default. As FEL pulses are collected the statistical properties are defined as ensemble averages over a large number of individual events, with the assumption that each event was created by different statistically independent electron bunches.

For each SASE pulse, the measured beam intensity at two pixels locations at position  $r_1, r_2$  are  $I_1$  and  $I_2$ . If the light at positions  $r_1, r_2$  is correlated then for first order the fields will interfere generating visibility fringes. Our interest is to analyse the second-order intensity cross-correlation term which can be expressed as [10]

$$g_2(r_1, r_2) = \frac{\langle I_1 I_2 \rangle}{\langle I_1 \rangle \langle I_2 \rangle} \quad (1)$$

where the angular brackets  $\langle \dots \rangle$  denote an ensemble average over a large number of individual pulses.

The statistical properties of the second-order intensity correlation depend on the type of radiation source. For fully coherent (laser) source,  $g_2(r_1, r_2)=1$ . For chaotic source,  $g_2(r_1, r_2)>1$ . Moreover, in the case of a chaotic source, if we define the total intensity of each pulse as  $I$ , the probability distribution of  $I$  follows gamma-function distribution [10].

$$P(I) = \frac{M^M}{\Gamma(M)} \left(\frac{I}{\langle I \rangle}\right)^{M-1} \exp\left(-M \frac{I}{\langle I \rangle}\right) \quad (2)$$

For coherent laser radiation,  $P(I)$  obeys the well-known normal or Gaussian distribution [10]

\* Work supported by Shanghai Sailing Program (18YF1428700)

<sup>†</sup> lichunlei@zjlab.org.cn

$$P(I) = \frac{1}{\sqrt{2\pi\sigma^2}} \exp\left(-\frac{(I - \langle I \rangle)^2}{2\sigma^2}\right) \quad (3)$$

Assuming a quasi-monochromatic pulsed source with finite cross-section, and the propagating fields arrive at two space points  $P_1$  and  $P_2$  can be written as  $E(p_1, t_1)$  and  $E(p_2, t_2)$ . Due to the fact that the source is pulsed, the first-order mutual coherence function (MCF) or mutual intensity of the light can be described as an ensemble average [10] in both space and time:

$$\Gamma_{12}(p_1, p_2; t_1, t_2) = \lim_{N \rightarrow \infty} \frac{1}{N} \sum_{n=1}^N E_n^*(p_1, t_1) E_n(p_2, t_2) \quad (4)$$

The average intensity of the beam averaged over both space and time is simply

$$\langle I(p_n, t_n) \rangle = \lim_{N \rightarrow \infty} \frac{1}{N} \sum_{n=1}^N |E_n(p_n, t_n)|^2 \quad (5)$$

Combining Eqs. (4) and (5), the normalized mutual coherence function or complex degree of coherence can be expressed as

$$\gamma_{12} = \frac{\Gamma_{12}(p_1, p_2; t_1, t_2)}{\sqrt{\langle I(p_1, t_1) \rangle} \sqrt{\langle I(p_2, t_2) \rangle}} \quad (6)$$

The measured magnitude of  $\gamma_{12}$  (visibility) evaluated when  $t_1=t_2$  is often used to calculate the size of an SR beam using the Van Cittert-Zernike theorem [11-12].

In our case, assuming the SASE X-ray radiation thermal obeys Gaussian statistics and that the beam is both fully polarized and cross-spectrally pure, the normalized intensity correlation function becomes [7, 10]

$$g_2(r_1, r_2) = 1 + \frac{|\gamma_{12}|^2}{M} \quad (7)$$

where  $M$  is the modes number representing total degrees of freedom, and  $\gamma_{12}$  is again the complex degree of spatial coherence which depends on detector separation. In general,  $M = M_s M_t$ , where  $M_s$  and  $M_t$  are the spatial and temporal degrees of freedom, respectively. Note that Equation 7 states that  $|\gamma_{12}|$  can be deduced by measurement of  $g_2(r_1, r_2)$ . This is an important result since measurement of  $g_2(r_1, r_2)$  tends to be immune from vibration effects that reduce contrast in measurements of  $|\gamma_{12}|$ .

## SIMULATIONS AND EXPERIMENTAL RESULTS

In order to explore the second order intensity correlation of FEL SASE pulses at SXFEL, 700 pulses were simulated with 299 longitudinal slices along pulse using Genesis 1.3. Spectral bandwidth  $\Delta\omega/\omega$  for each pulse is  $1 \times 10^{-3}$ . The radiation field is evaluated after amplification in the FEL undulators with a total length 28m. Machine parameters for the simulation are shown in Table 1 [13].

The total bandwidth was then filtered to  $1 \times 10^{-5}$  with a central wavelength of 8.8nm to increase the coherence time  $\tau_c \sim 1/(\Delta\omega/\omega)$ . The SASE beam intensity in this bandwidth was evaluated for second-order intensity correlation calculations and statistical analysis.

For the analysis, the intensity distribution for each pulse was first projected in the horizontal (x) and vertical

(y) direction and then the second-order intensity correlation functions were calculated according to Eq. (1).  $g_2(x_1, x_2)$  and  $g_2(y_1, y_2)$  are shown in Fig. 2(a) and Fig. 2(b), respectively. For the case shown, the second order intensity correlation value  $1.761 \leq g_2(x_1, x_2) \leq 1.853$ , and  $1.747 \leq g_2(y_1, y_2) \leq 1.825$ , i.e. the beam was nearly 'round' in cross-section.

Table 1: SXFEL Simulation Parameters

Parameter	Value	Unit
Beam Energy	840	MeV
Peak Current	500	A
Nor. Emittance	2.0	mm·mrad
Slice Energy Spread	1.5e-4	
Bunch Length	<1.0	ps (FWHM)
Bunch Charge	0.5	nC
FEL wavelength	8.8	nm
FEL power	>100	MW

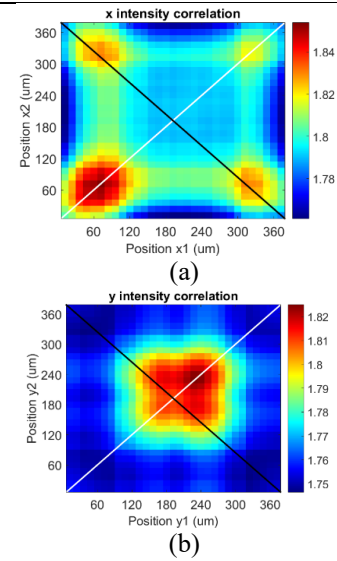


Figure 2: Intensity-intensity cross-correlation functions from Eq. 1: (a)  $g_2(x_1, x_2)$  and (b)  $g_2(y_1, y_2)$ .

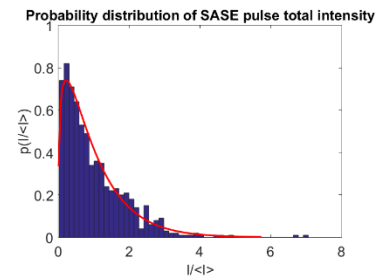


Figure 3: Histogram of probability distribution  $p(I \langle I \rangle)$  for 700 SASE pulses. The red line represents a numerical fit to the gamma-function Eq. (2) with  $M=1.279$ .

A histogram of the SASE pulse intensities is shown in Fig. 3. For SASE process, the radiation is generated stochastically in the electron bunch by shot noise. In general, each SASE pulse contains a finite number of longitudinal modes with no inherent phase locking between modes. As a result, the spatial and temporal structure of the FEL pulse fluctuates from shot to shot longitudinally the SASE source is chaotic from a statistical point of view. The

Content from this work may be used under the terms of the CC BY 3.0 licence (© 2019). Any distribution of this work must maintain attribution to the author(s), title of the work, publisher, and DOI

resulting histogram was fitted by a gamma function (Eq. (2)) with mode number  $M=1.279$ .

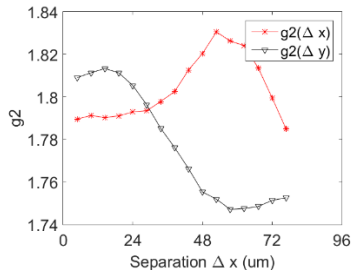


Figure 4: Second order intensity correlation values  $g_2(\Delta x)$  and  $g_2(\Delta y)$  take along the black diagonal lines in Figure 2(a) and 2(b).

As expected, when the separation distance  $\Delta x$  between pixels increases, the correlation function  $g_2(\Delta x)$  decreases, in this case from 1.81 to 1.75.  $\gamma_{12}$  decrease from 1.018 to 0.979 calculated from Eq. (7). Due to gamma fit error, it comes the case  $\gamma_{12} = 1.018 > 1$ . Nevertheless, From Fig. 5  $g_2(\Delta x)$  first increases to 1.83 and then decreases to 1.78. This effect could be an artefact of the simulation and needs further investigation.

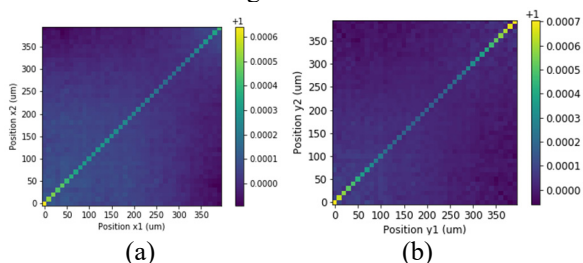


Figure 5: Second order intensity correlation function (a)  $g_2(x_1, x_2)$  and (b)  $g_2(y_1, y_2)$  for a phase-locked laser.

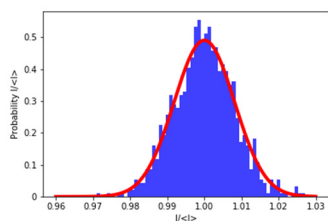


Figure 6: Histogram of probability distribution  $p(I < I>)$  for the phase-locked Ti:sapphire laser. The red line represents fit result by Gaussian function.

In order to compare the statistical properties of SASE pulses with a laser beam, 1000 pulses of phase-locked 800nm Ti:sapphire laser light with 15nm bandwidth were similarly captured on a CCD camera (Basler scA640-70gm). The beam size at the camera was  $\sim 400\mu\text{m}$  in diameter. The beam intensity was again projected into horizontal direction with the second-order intensity correlation shown in Fig. 5. The results show that  $0.9999 \leq g_2(x_1, x_2) \leq 1.0006$ , and  $0.9999 \leq g_2(y_1, y_2) \leq 1.0007$  demonstrating the Ti:sapphire light is fully coherent in the transverse plane. The normalized statistical distribution for beam intensity is shown in Fig. 6. In this case the data fits well

to a Gaussian distribution with average value 1.0 and standard deviation 0.008.

## CONCLUSION

Second order intensity correlation functions of simulated SASE pulses for the Shanghai Soft X-Ray FEL were investigated and compared with measurement from a Ti:Sapphire laser. The results show the SASE radiation has the properties of a chaotic source with  $M=1.28$  in the transverse plane, which agrees well with theory. Both the second intensity correlation and statistical properties are significantly different from a phase-locked Ti:sapphire laser.

## ACKNOWLEDGEMENTS

The first author would like to thank Jeff Corbett and Toshi Mitsuhashi for interesting discussions, Duan Gu for python coding support, and funding support from Shanghai Sailing Program (18YF1428700).

## REFERENCES

- [1] Eberhard J. Jaeschke, Shaikat Khan, Jochen R. Schneider and Jerome B. Hastings, "Synchrotron Light Sources and Free-Electron Lasers", Springer, 2016, pp. 825.
- [2] Roy J. Glauber, "The Quantum Theory of Optical Coherence", Physical Review, Vol.130, No.6, 1963, pp. 2529-2534.
- [3] F.T. Arecchi, E. Gatti, and A. Sona, "Time Distribution of Photons from Coherent and Gaussian Sources", Physics Letters, Vol.20, No.1, 1966, pp. 27-29.
- [4] R. Hanbury Brown and R. Q. Twiss, "Correlation Between Photons in Two Coherent Beams of Light", Nature, Vol.177, No. 4497, 1956, pp. 47-49.
- [5] R. Hanbury Brown and R. Q. Twiss, "A Test of a New Type of Stellar Interferometer on Sirius", Nature, Vol.178, No. 4541, 1956, pp. 1046-1048.
- [6] W. J. Corbett and T. M. Mitsuhashi, "Intensity Interferometer to Measure Bunch Length at SPEAR3", in *Proc. IPAC'17*, Copenhagen, Denmark, May 2017, pp. 60-63. doi:10.18429/JACoW-IPAC2017-MOOCB3
- [7] Sanghoon Song et al., "Intensity Interferometry Measurement with Hard X-ray FEL Pulses at the Linac Coherent Light Source", Proc. of SPIE, Vol. 9210, 2014, pp. 92100M-1.
- [8] O. Yu. Gorobtsov et al., "Statistical Properties of a Free-Electron Laser revealed by Hanbury Brown-Twiss Interferometry", Physical Review A 95, 2017, pp. 023843-1.
- [9] O.Yu. Gorobtsov, et al., "Seeded X-ray free electron laser generating radiation with laser statistical properties", Nature Communications, 9:4498, 2018, pp. 1-5.
- [10] J. Goodman, "Statistical Optics", John Wiley & Son, Wiley Classics Library Edition Published 2000, pp. 237-255.
- [11] T. Mitsuhashi, "Twelve Years of SR Monitor Development", in *Proc. 11<sup>th</sup> Beam Instrumentation Workshop (BIW04)*, Knoxville, Tennessee, May 3-6, 2004, AIP, 732, pp. 5-11.
- [12] C. L. Li et al., "Double-slit Interferometer Measurements at SPEAR3", in *Proc. IPAC'16*, Busan, Korea, May 2016, pp. 368-370. doi:10.18429/JACoW-IPAC2016-MOPMR054

- [13] D. Wang, “Soft X-ray Free Electron Laser at SINAP”, in *Proc. 7th Int. Particle Accelerator Conf. (IPAC'16)*, Busan, Korea, May 2016, pp. 1028-1031.  
doi:10.18429/JACoW-IPAC2016-TUZA01